

Stabilities of large sodium clusters for different atomic arrangements

M. D. Glossman, J. A. Alonso, and M. P. Iñiguez

Departamento de Física Teórica, Universidad de Valladolid, E 47011, Valladolid, Spain

(Received 12 May 1992; revised manuscript received 25 August 1992)

We have used density-functional theory and the spherically averaged pseudopotential (SAPS) model to study the relative stabilities of large sodium clusters with different atomic arrangements. Starting with perfect crystalline clusters with filled atomic shells, we find that small distortions of the geometry strongly enhance their stability. However, in the size range studied in this paper ($N \leq 340$) the distorted-crystalline structures are not the absolute energy minima. These are, instead, noncrystalline structures obtained by energy minimization without any structural constraints. In particular, noncrystalline clusters with enough electrons to fill electronic shells are the most stable ones. The crossover between magic numbers of electronic origin (clusters with filled electronic shells) and magic numbers of atomic origin (crystalline structures with filled atomic shells) has not yet taken place in the size range studied here and should occur for larger sizes.

I. INTRODUCTION

The electronic-shell model has proved very useful in understanding the size variation of many properties of metallic clusters.¹ In this model the valence electrons move in a smooth spherically symmetric potential. The simplicity of the model makes it very attractive from a theoretical point of view. Calculations initially performed in the size range below 100 atoms¹⁻⁶ have progressively been extended to clusters with a few hundred⁷⁻⁹ or even a few thousand atoms.¹⁰⁻¹² Jellium,^{1-6,12} Wood-Saxon,¹⁰ and infinite square-well¹³ effective one-electron potentials have been used in the resolution of the Schrödinger equation. None of these potentials accounts for the discrete nature of the ions and consequently the one-electron eigenvalues and electronic distributions are independent of the detailed geometrical arrangement of the atoms. The supershell structure observed in alkali-metal clusters^{14,15} and the transition from electronic magic numbers to geometrical magic numbers (icosahedral or cuboctahedral) reported for sodium clusters¹⁶ are two interesting topics in the large size domain.

Evidently, the geometry has to be taken into account explicitly to investigate this transition. A full-scale calculation for large clusters including geometrical effects is a very demanding task. Consequently, simpler approaches have been explored. First-order and second-order perturbation theory have been used by Maiti and Falicov¹³ and by Clemenger,¹¹ respectively, to account for the deviations of the ionic background potential from the smooth potential of the jellium-type models. Maiti and Falicov have concluded that geometrical effects overtake electronic-shell effects when the number of atoms in the cluster becomes larger than a critical value N_c of about 100. In other words, that the most stable clusters are those that correspond to closed electronic shells for N smaller than about 100, and to specially stable polyhedral clusters for N larger than about 100. This criti-

cal number is too small compared with the value induced from experiment ($N_c \approx 1500$).¹⁶ The calculation of Maiti and Falicov is similar, in essence, to the SAPS (spherically averaged pseudopotential) model that we have used in several previous papers,^{3,17-20} although it contains some additional simplifying assumptions. In the present work we use the SAPS model to analyze the question if the critical number could be as small as predicted by Maiti and Falicov. To this end we have studied the stabilities of sodium clusters with up to 340 atoms for different geometric arrangements: those are the crystalline body-centered-cubic and face-centered-cubic structures, the multilayered icosahedra, and the geometries that result from the unconstrained relaxation of initial random atomic arrangements. In Sec. II we present the calculational methods and compare the relative stabilities of the different structures. In Sec. III we study the competition between magic numbers of electronic and atomic origin. Finally, the conclusions are presented in Sec. IV.

II. STABILITY OF DIFFERENT GEOMETRICAL STRUCTURES

A. SAPS model

In general, the ground-state electron density $\rho(\mathbf{r})$ and the energy of a cluster of N atoms placed at given positions $\{\mathbf{R}_j\}_{j=1,\dots,N}$ are obtained by minimizing the energy functional $E[\rho;\{\mathbf{R}_j\}]$ with respect to $\rho(\mathbf{r})$. In the spherically averaged pseudopotential (SAPS) model^{3,17} this is achieved in practice by self-consistently solving the Kohn-Sham equations of the density-functional formalism²¹ under the assumption that the total three-dimensional external pseudopotential due to the ionic background

$$V_{\text{ext}}(\mathbf{r}) = \sum_{j=1}^N v(|\mathbf{r} - \mathbf{R}_j|) \quad (1)$$

is replaced by its spherical average $V_{\text{ext}}^{\text{av}}(r)$ about the center of mass of the cluster. Furthermore, if one is interested in the equilibrium geometry of the cluster, then the total energy $E[\rho; \{\mathbf{R}_j\}]$ must also be minimized with respect to the set of ion positions $\{\mathbf{R}_j\}$. The total energy at temperature $T = 0$ K can be written as a sum of several terms (Hartree atomic units are used through the paper unless explicitly stated)

$$E[\rho; \{\mathbf{R}_j\}] = G[\rho] + \frac{1}{2} \int \int \frac{\rho(\mathbf{r})\rho(\mathbf{r}')}{|\mathbf{r} - \mathbf{r}'|} d\mathbf{r} d\mathbf{r}' + \int V_{\text{ext}}^{\text{av}}(r) \rho(\mathbf{r}) d\mathbf{r} + \frac{1}{2} \sum_{j \neq j'} U(|\mathbf{R}_j - \mathbf{R}_{j'}|). \quad (2)$$

The first term, $G[\rho]$, is the sum of the kinetic, exchange, and correlation energies of the electrons, the second term gives the classical electron-electron interaction, the third term is the interaction of the electronic cloud with the external SAPS pseudopotential, and the last term gives the ion-ion interaction. In summary, the electronic cloud only feels the spherical-average component of the external ionic pseudopotential, but the geometrical structure of the cluster is fully taken into account in the ion-ion interaction term. Steepest-descent^{17–20} and simulated annealing techniques²² have been used to search for the local and global energy minima.

B. Simplification of the SAPS model

Maiti and Falicov¹³ have performed calculations for sodium clusters in a spirit similar to the SAPS model. For some clusters the geometric structure was assumed to be the same as in a crystal with body-centered-cubic (bcc) structure or face-centered-cubic (fcc) structure. The study was restricted to clusters with a number of atoms such that the cluster only contains closed coordination shells of atoms about the center. For bcc clusters with an atom at the center, the shell closing numbers are $N = 9, 15, 27, 51, 59, 65, 89, 113, 137, 169, 181, \dots$ and for fcc clusters with an atom at the center $N = 13, 19, 43, 55, 79, 87, 135, 141, 177, 201, \dots$. These authors have also studied fcc clusters centered on interstitial lattice positions of high symmetry. In addition, they have considered a second set of clusters with a number of atoms $N = 8, 18, 20, 34, 40, 58, 68, 90, 92, 106, 132, 138, 168, 186, 196, 198, 232, \dots$, which are the well-known clusters with closed electronic shells.¹ For those clusters the geometrical structure was calculated by minimization of the total energy $E[\rho; \{\mathbf{R}_j\}]$ with respect to the ion positions. In a plot of the total energy as a function of cluster size, the “hulls” of minimum energy were drawn separately for the two sets of clusters, that is, for the electronic- and atomic-shell numbers. It was then observed that the hull of electronic-shell numbers is below the other for N smaller than about 100 and above it for N larger than about 100. From this it was concluded that $N_c \approx 100$ marks the crossover of cluster stability from electronic magic numbers to atomic magic numbers.

The crossover observed in the experiments of Martin *et al.*¹⁶ is much larger ($N_c \approx 1500$) and we suspect that the underestimation of N_c in the work of Maiti and Falicov is due to an additional approximation in their calculation, as compared to the original form of the SAPS model:^{3,17} the shortcoming is that the electron density is not self-consistent with the ion background distribution. The electron density was in each case that calculated for a simple infinite spherical potential well of appropriate size and containing the proper number of electrons. The interaction of this electron density ρ_0 with the ion background pseudopotential (actually, with its spherical average) was introduced perturbatively, that is, evaluating $\int V_{\text{ext}}^{\text{av}}(r)\rho_0(\mathbf{r})d\mathbf{r}$, where $\rho_0(\mathbf{r})$ is the density of the square-well problem. In summary, the energy of the cluster defined by the set of ionic positions $\{\mathbf{R}_j\}$ was given by [compare with Eq. (2)]

$$E[\rho^0; \{\mathbf{R}_j\}] = G[\rho^0] + \frac{1}{2} \int \int \frac{\rho^0(\mathbf{r})\rho^0(\mathbf{r}')}{|\mathbf{r} - \mathbf{r}'|} d\mathbf{r} d\mathbf{r}' + \int V_{\text{ext}}^{\text{av}}(r) \rho^0(\mathbf{r}) d\mathbf{r} + \frac{1}{2} \sum_{j \neq j'} U(|\mathbf{R}_j - \mathbf{R}_{j'}|). \quad (3)$$

This simplification can affect the results since there is evidence that some of the minima and shoulders of the radial electron density are closely correlated with the position of the atomic shells.²³ This correlation is absent if one uses the density of the spherical-well problem, where the only modulations of the electron density are due to electronic shells. We suspect that the lack of self-consistency influences the conclusions concerning the quantitative value of the crossover size from electronic-shell to atomic-shell magic numbers. In fact, this shortcoming was also pointed out by Maiti and Falicov.¹³

To check this point we have performed SAPS calculations for sodium clusters in which the self-consistency between the SAPS pseudopotential and the electron density is preserved. To this end, we separate our study in two parts. In the first step we concentrate on the study of the preferred geometrical arrangement as a function of cluster size, without the interference of electronic-shell closing effects. For this purpose we use a simplification of the density-functional formalism which permits faster calculations. Then in a second step we discuss the additional stabilization effects due to electronic-shell closing.

C. Comparison of geometric structures

The search for the equilibrium geometry of each cluster has been performed by first generating a set of random initial geometries and then relaxing the ion positions by the steepest-descent method for the total energy, that is, by moving a little of each atom in the direction of the net force acting on it. At each step in the relaxation process, the electron density, energy, and forces are recalculated, and the process is iterated until the forces on all atoms vanish. We are well aware of the insurmountable difficulties to find the absolute-energy minimum for a medium

size or large cluster. This is because the number of relative energy minima in the energy hypersurface escalates rapidly with the number of atoms in the cluster.²⁴ In fact, the number of relative minima with energies very close to that of the absolute minimum can be large, and one is likely to be trapped in one of those relative minima. Of course, the search for the lowest minimum is made more efficient by increasing the number of trial initial configurations of the cluster. In our case we estimate that the number of initial configurations was large enough to allow us to reach a minimum close in energy to the absolute minimum. Other efficient ways to optimize the structure is to use simulated annealing techniques,²² although the computations become very tedious and the method is not suitable for the broad study, involving many large clusters, that we perform in this paper.

The growth pattern of alkaline-metal clusters for sizes $N < 100$ has been discussed in previous papers,^{17,24,25} and we only recall here the most salient features. The clusters are not small fragments of a crystal. The atoms are arranged in spherical layers. There is a small dispersion in the radial coordinate of the atoms within each layer, but the layers are well separated from each other. Two examples of this layering are shown in Figs. 1(d) and 2(d) for Na_{51} and Na_{55} , respectively, which will be fully discussed below. We should also mention that the cluster strongly reconstructs as it grows. This pattern of growth, which extends at least up to the largest clusters studied in the present paper ($N \leq 340$), is very different from that which would result from the successive filling of coordination shells around an atom in a perfect crystal.

Even if our calculations clearly demonstrate that in this size range the lowest-energy structures are not derived from a piece of the crystalline bulk lattice (this is fully discussed in the rest of the paper), it is nevertheless interesting to know how different the energies of clusters with crystallinelike structures are from those of the lowest-energy (noncrystalline) structures. For this purpose we have also performed calculations for some crystalline geometries (bcc and fcc). In this case the cluster is a spherical piece cut from the perfect lattice; that is, we only have considered clusters with closed atomic coordination shells around the center. The center is a lattice site for the bcc clusters. For the fcc structure we have taken two series of clusters. The cluster center is a lattice site in the first series (I), and in the other (II) the cluster center coincides with the center of the conventional cube. Finally we have also studied icosahedral clusters; both experiments¹⁶ and theoretical calculations²⁶ suggest the relevance of icosahedral structures in the size range of interest here. The list of the crystalline and icosahedral clusters studied is given in Table I.

Since in this section we are only interested in comparing the relative stabilities of clusters with different geometrical structures and we want to deal with fairly large sizes (N up to ≈ 340), it is enough for our purposes to introduce a convenient simplification in the density-functional formalism. Instead of treating the electronic kinetic energy exactly by the Kohn-Sham method,²⁷ we use an extended Thomas-Fermi method, including the gradient correction to the kinetic energy, completely for-

TABLE I. Number of atoms in the different crystalline and icosahedral clusters studied.

Geometry	Number of atoms
bcc	9, 15, 27, 51, 59, 65, 89, 113, 137, 169, 181, 307
fcc(I) ^a	13, 19, 43, 55, 79, 87, 135, 141, 177, 201, 321
fcc(II) ^b	14, 38, 68, 92, 116, 164, 188, 236, 298, 322
Icosahedral	13, 55, 147, 309

^aCentered on an atom.

^bCentered on the center of the conventional cube.

mulated in terms of the electron density. Our kinetic-energy functional is then

$$T[\rho] = \frac{3}{10}(3\pi^2)^{2/3} \int \rho^{5/3} d\mathbf{r} + \frac{\lambda}{8} \int \frac{|\nabla\rho|^2}{\rho} d\mathbf{r}, \quad (4)$$

where the first term is the Thomas-Fermi approximation²¹ and the second is the Weizsäcker correction.²⁸ Choosing for λ the value $\lambda = 0.5$ gives results for the total energies and the geometries of sodium clusters in good agreement to those obtained from full Kohn-Sham calculations.^{23,29} The exchange and correlation energies, E_x and E_c , have been expressed in the local-density approximation due to Dirac³⁰ and Wigner,³¹ respectively,

$$E_x[\rho] = -\frac{3}{4} \left(\frac{3}{\pi}\right)^{1/3} \int \rho^{4/3} d\mathbf{r}, \quad (5)$$

$$E_c[\rho] = -\int \frac{0.44\rho}{7.8 + (4\pi\rho/3)^{-1/3}} d\mathbf{r}. \quad (6)$$

The sum of $T[\rho]$, $E_x[\rho]$, and $E_c[\rho]$ forms the part labeled $G[\rho]$ in Eq. (2). The rest of the energy terms are the same ones appearing in that equation. The ion pseudopotential that we have used is the empty-core pseudopotential due to Ashcroft,³² which is zero inside the core radius r_c and purely Coulombic outside, and the ion-ion interaction is given by the repulsion energy between pointlike ions. The core radius $r_c = 1.74$ a.u. is taken from previous papers.¹⁷

In Fig. 1 we show histograms corresponding to the radial distribution of the ions in Na_{51} with bcc structure for several specific situations. Of course the radial distributions are measured with reference to the cluster center. Panel 1(a) corresponds to a perfect bcc cluster with interatomic distances equal to those in the bulk crystal at low temperature (lattice constant $a = 7.987$ a.u., nearest-neighbor distance $d_{nn} = 0.866a$).³³ If the lattice constant a is optimized by minimization of the total energy we obtain the radial distribution of panel 1(b); in this way we observe a slight contraction of the volume of the cluster. Similar results are presented for fcc Na_{55} in Fig. 2. In this case panel 2(a) is such that the nearest-neighbor distance has the same value as for the bulk bcc lattice. Optimization of the nearest-neighbor distance leaves the cluster practically unchanged [see panel 2(b)]. The different behavior of bcc and fcc clusters can be understood from the fact that for equal nearest-neighbor distances $d_{nn}(\text{bcc}) = d_{nn}(\text{fcc})$, the Wigner-Seitz sphere

radius of the fcc lattice [$R_{WS}(fcc) = 0.5526d_{nn}$] is already slightly smaller than the Wigner-Seitz radius of the bcc lattice [$R_{WS}(bcc) = 0.5685d_{nn}$]. Panels 1(c) and 2(c) of these figures will be discussed later. Finally, in panels 1(d) and 2(d) we give the structures obtained by a complete steepest-descent minimization of the energy without any structural constraints, starting from a number of random initial configurations; in other words, these are the lowest-energy equilibrium structures predicted by the SAPS model. Compared to the crystalline clusters we observe a decrease in the number of atomic layers, which then become more populated. Also these shells have a thickness between 0.5 a.u. and 1 a.u. Since the distribution of atoms in these clusters bears no relation to that in the crystalline ones, we shall call them noncrystalline clusters.

We have collected the energies for the series of bcc and fcc (types I and II) clusters with optimized lattice constants. The results are compared in Fig. 3 with the energies of the fully optimized noncrystalline clusters (lowest-energy structures) of the same size. In other words, the number of atoms in the noncrystalline clusters is also taken from Table I. We observe that the clusters with crystalline structures are less stable than the fully optimized, or noncrystalline clusters, indicating that perfect

crystalline structures are very unlikely in this size range. This provides a first indication that the self-consistency between ionic potential and electron density is important in the analysis of structural effects.

There are, however, other structures which could be competitive with the noncrystalline clusters, but unlikely to be found from the steepest-descent calculations starting with random geometries. Those new structures can be obtained by the steepest-descent relaxation of the perfect crystalline clusters with optimized nearest-neighbor distance. It is expected that the perfect crystalline clusters are near a local energy minimum of the energy hypersurface corresponding to a distorted crystallinelike structure, and that by the steepest-descent relaxation the cluster will easily fall into that minimum. The expectation is in fact correct. We show the results in panel (c) of Figs. 1 and 2 for Na_{51} and Na_{55} , respectively. The number of atomic shells and their population are identical to those in the perfect crystalline clusters of the same size but there are small radial displacements (inwards or outwards) of the shells. The displacements are in the direction so as to concentrate the atoms into a smaller number of more populated shells, although the extreme situation of panel (d) of Figs. 1 and 2 has not yet been achieved. Since the population of the different shells coin-

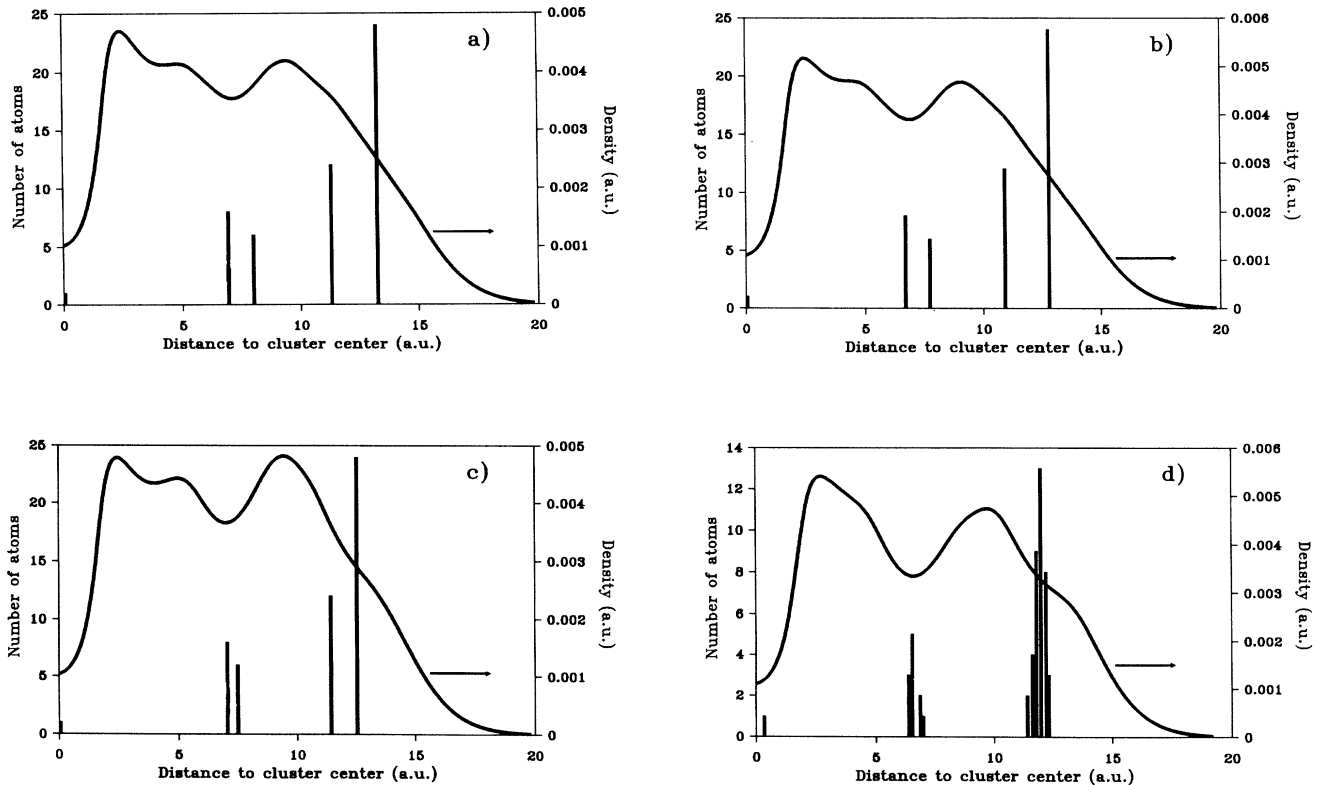


FIG. 1. Histograms showing the radial distribution of atoms (with respect to the cluster center) in Na_{51} : (a) perfect bcc structure with the bulk interatomic distance; (b) perfect bcc structure with optimized nearest-neighbor distance; (c) distorted-crystalline structure obtained by steepest-descent relaxation of case (b); (d) lowest-energy structure, obtained by steepest-descent minimization of the energy starting from several random initial geometries (notice the different scale). The electron density is also plotted in each case as a continuous curve.

cides with the populations in the perfect crystalline clusters and those shells are still clearly defined, we call those structures distorted-crystalline structures.

If we repeat the comparison of Fig. 3, but now using the distorted-crystalline clusters instead of the perfect crystalline ones we arrive at Fig. 4. Evidently, the distorted-crystalline structures become more and more competitive with the noncrystalline ones as the cluster size increases. In this plot there are a few cases in which the distorted-crystalline structures are equally stable and, for $N > 130$, even more stable than the noncrystalline clusters of the same size. For instance, the distorted fcc structures are degenerate with the disordered structures for $N = 59, 113$, or 307 , and the distorted-crystalline clusters are more stable than the disordered ones for $N = 137$ or 236 . This simply means that the steepest-descent method does not explore the full energy hypersurface and that the cluster becomes trapped in different local minima depending on the initial atomic configuration. The very stable distorted-crystalline clusters $N = 137$ or 236 cannot be obtained by the steepest-descent method starting with a random initial arrangement of the atoms; those can be obtained, instead, by the relaxation of educated geometries (the perfect crystalline clusters) rather similar to the final one. This observa-

tion gives additional support to our strategy of investigating the equilibrium structures by the steepest-descent relaxation of "two" different types of initial geometries: (a) random atomic arrangements, and (b) educated crystalline geometries. Just restricting our study to one of the two sets would have the consequence of missing a lot of interesting low-energy structures. The search for the global minimum can be improved if we use the technique of simulated annealing.²² In such a case the computations require a lot more time and a broad study as we have performed in the present paper becomes impractical.

By comparing the energies of the distorted bcc and distorted fcc clusters we find no evidence for the dominance of one structure over the other. In the same figure we have also plotted the results for the Mackay series of icosahedral clusters ($N = 13, 55, 147, 309, \dots$).³⁴ In this case we have also performed a steepest-descent relaxation of the perfect structure, although we have found that the distortions are very small. The icosahedral structures are very competitive. This can also be seen in Fig. 5 for Na_{19} . In 5(a) we show an isomer practically degenerate with the most stable structure. This isomer is a distorted double icosahedron, more spherical than the perfect double icosahedron, which is shown for comparison in 5(b).

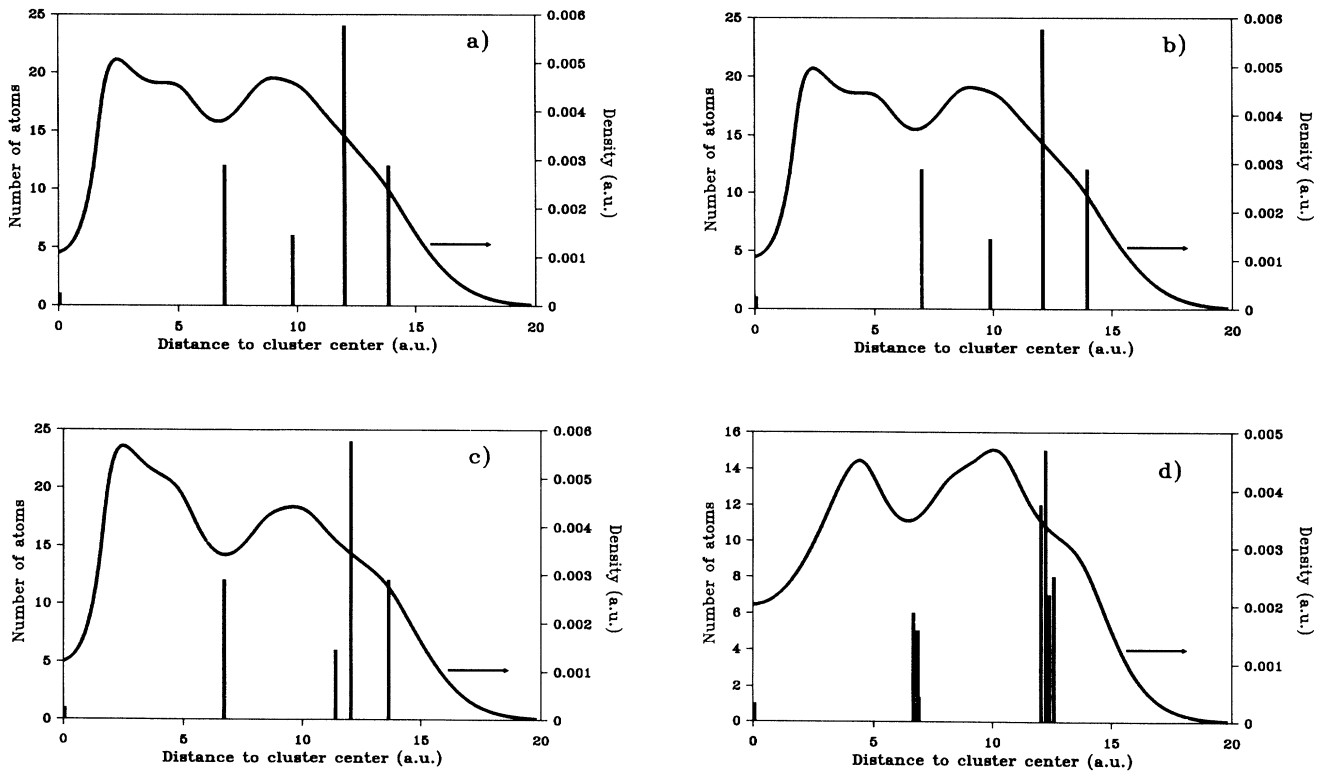


FIG. 2. Histograms showing the radial distribution of atoms (with respect to the cluster center) in Na_{55} : (a) perfect fcc structure with a nearest-neighbor distance equal to that in the bulk bcc crystal; (b) perfect fcc structure with optimized nearest-neighbor distance; (c) distorted-crystalline structure obtained by steepest-descent relaxation of case (b); (d) lowest-energy structure, obtained by steepest-descent minimization of the energy starting from several random initial geometries (notice the different scale). The electron density is also plotted in each case as a continuous curve.

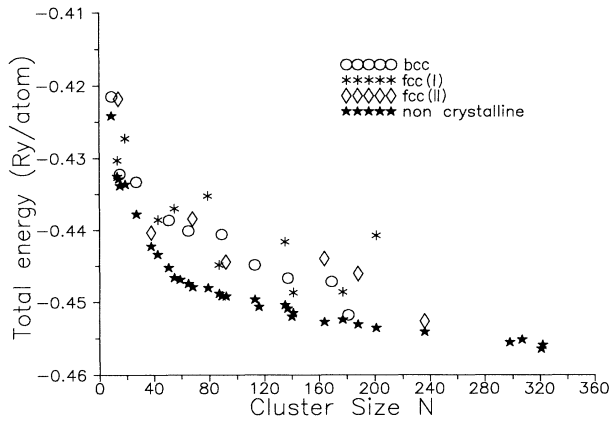


FIG. 3. Energies of perfect bcc and fcc clusters with optimized interatomic distances as a function of size, compared to the lowest-energy (or noncrystalline) structures. The cluster center in type-I fcc clusters is an atom, whereas in type II it is the center of the conventional cube.

The increased sphericity is due to the SAPS approximation. The double icosahedron is the lowest energy structure of Lennard-Jones clusters with $N = 19$.³⁵

In summary the results of Fig. 4 indicate a strong competition between icosahedral, distorted-crystalline (bcc and fcc) and noncrystalline clusters, with a slight dominance of the noncrystalline clusters, nonexempt of a number of exceptions. The energy curve we could draw joining the energy points of noncrystalline structures would be smooth. This is not the case for the distorted-crystalline structures. The latter would be even less smooth if we had included bcc or fcc clusters with open atomic shells. Actually there is a considerable loss of stability for those open atomic-shell crystalline structures.^{3,36}

An analysis of the interatomic distances in the perfect crystalline clusters is presented in Fig. 6. Here we have plotted the optimized nearest-neighbor distance d_{nn} as a function of cluster size. There is a tendency for d_{nn} to increase with N . In the bcc clusters d_{nn} has reached a

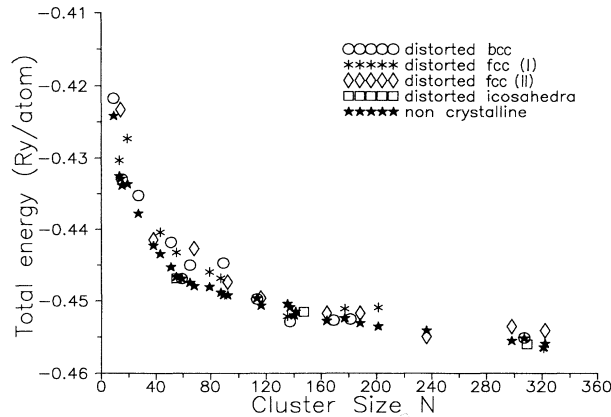


FIG. 4. Energies of distorted-crystalline bcc and fcc clusters and distorted icosahedral clusters as a function of size, compared with the (fully optimized) noncrystalline clusters.

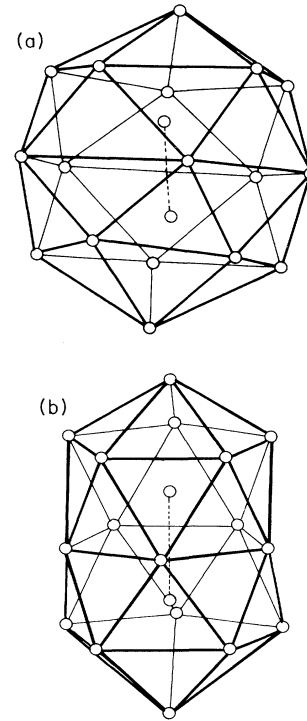


FIG. 5. (a) Distorted double icosahedron, which is the most stable structure of Na_{19} . (b) Perfect double icosahedron.

value $d_{nn} = 6.87$ a.u. for $N = 307$. This is only a little bit smaller than the experimental nearest-neighbor distance in the bulk solid ($d_{nn} = 6.91$ a.u.),³³ which is indicated by the horizontal line in the figure. The small difference is due to the finite size. The large fcc clusters have $d_{nn} = 7.16$ a.u. The relation between the volume per atom Ω and d_{nn} is $\Omega = 0.7698d_{nn}^3$ in the bcc lattice and $\Omega = 0.7071d_{nn}^3$ in the fcc lattice. Then, the calculated volumes per atom of large clusters are $\Omega(\text{bcc}) = 249.6$ a.u.³ and

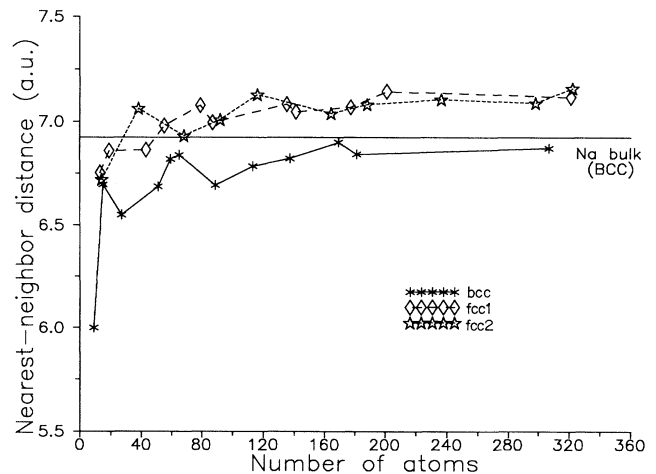


FIG. 6. Optimized nearest-neighbor distance of perfect crystalline clusters as a function of cluster size. The horizontal line indicates the value in the bulk (bcc) crystal.

$\Omega(\text{fcc}) = 259.7 \text{ a.u.}^3$. These should be compared with the experimental $\Omega(\text{bulk}) = 254.5 \text{ a.u.}^3$.

An interesting question the reader can ask is how large the distortions are in the distorted-crystalline clusters. The answer is provided in panels (a) and (b) of Fig. 7, which correspond to bcc and fcc (I) clusters, respectively. The magnitude plotted as a function of size is the ratio r_n/a , given separately for each atomic shell. a is the optimized lattice constant of the perfect crystalline cluster [for instance, clusters of Figs. 1(b) and 2(b)] and r_n ($n=1,2,3,\dots$) are the radii of the first, second, third, . . . coordination shells around the central atom in the distorted-crystalline clusters [for instance, those of Figs. 1(c) and 2(c)]. For perfect crystalline clusters the distances r_1, r_2, \dots exactly coincide with the first-neighbors distance, second-neighbors distance, etc., and the ratios $r_1/a, r_2/a, \dots$ are well-known universal numbers. The universal values are indicated by the arrows on

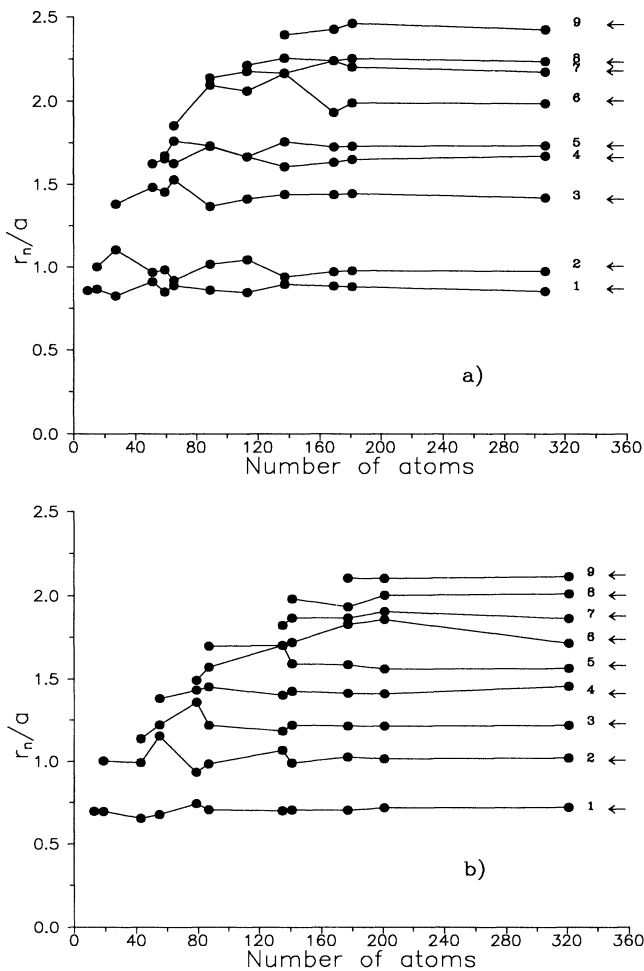


FIG. 7. Ratio r_n/a as a function of cluster size, plotted separately for each atomic shell. a is the optimized lattice constant of the perfect crystalline cluster and r_n ($n=1,2,\dots$) are the radii of the first, second, . . . coordination shells around the central atom in the distorted-crystalline cluster. Panel (a) is for bcc clusters and panel (b) for fcc (I) clusters.

the right-hand side of the figures. We conclude that the distortions are small (the values of r_n/a are close to the ideal ones), and that these distortions quickly become negligible as the cluster size increases. The distorted-crystalline clusters with N larger than ≈ 150 are practically undistorted.

III. INTRODUCTION OF ELECTRONIC-SHELL EFFECTS

A. Kohn-Sham method

In Sec. II we have obtained information about the competition between different ordered (crystalline or distorted crystalline) and disordered atomic structures as the cluster size grows. However, electronic-shell effects were absent from the calculations and consequently we cannot answer one of the main questions of interest, namely the competition between electronic magic numbers and atomic magic numbers. For this purpose we performed additional calculations using the Kohn-Sham formulation of density-functional theory.^{21,27} In this case the electron density is written as

$$\rho(\mathbf{r}) = \sum_i^{\text{occ}} |\Psi_i(\mathbf{r})|^2, \quad (7)$$

where the $\Psi_i(\mathbf{r})$ are one-electron orbitals, obtained by solving Schrödinger-like equations

$$\left\{-\frac{1}{2}\nabla^2 + V_{\text{eff}}(\mathbf{r})\right\} \Psi_i(\mathbf{r}) = E_i \Psi_i(\mathbf{r}), \quad (8)$$

in which the effective potential

$$V_{\text{eff}}(\mathbf{r}) = V_{\text{ext}}^{\text{av}}(\mathbf{r}) + \int \frac{\rho(\mathbf{r}')}{|\mathbf{r} - \mathbf{r}'|} d\mathbf{r}' + V_{\text{xc}}^{\text{LDA}}(\mathbf{r}) \quad (9)$$

is the sum of the external SAPS potential, the Hartree potential of the electronic cloud, and the exchange-correlation potential (in the local-density approximation). The cluster energy is then obtained in a standard way.^{21,27}

B. Results

Using the Kohn-Sham formulation we have performed again calculations for crystalline clusters, more precisely for distorted-crystalline clusters. The geometries, that is, the small distortions from the perfect crystalline structures, have been taken directly from our previous study in Sec. II and the Kohn-Sham calculations have been performed at those fixed distorted geometries since there is evidence that the extended Thomas-Fermi method and the full Kohn-Sham treatment of density-functional theory lead to very similar geometries in the SAPS approximation.²³ The results have been plotted in Fig. 8 where the distorted bcc, fcc, and icosahedral clusters are identified by the circles. A comparison with the distorted-crystalline clusters of Fig. 4 shows that the introduction of full quantum effects contributes to increase the stability of all the clusters, which now have more negative energies.

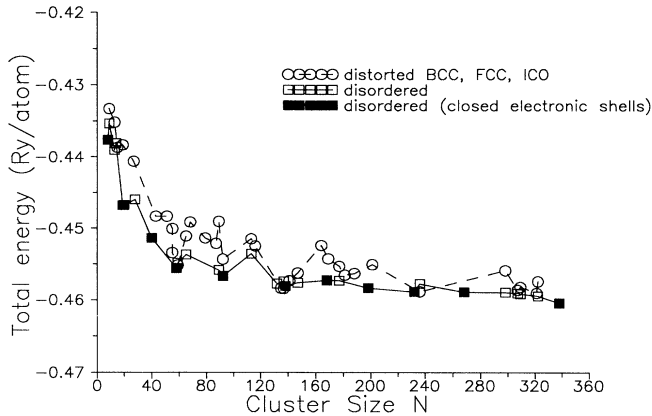


FIG. 8. Kohn-Sham energies of distorted-crystalline (bcc, fcc) and distorted icosahedral clusters compared with the noncrystalline clusters. The set of noncrystalline clusters now contains the well-known electronic magic numbers.

Figure 8 also shows the Kohn-Sham energies for the set of noncrystalline clusters, using again the geometries calculated in Sec. II. To this set, which originally was extracted from the numbers given in Table I, we have added several other clusters with a number of atoms corresponding precisely to the well-known electronic magic numbers:¹ 8, 20, 40, 58, 92, 138, 168, 198, 232, 268, 338. Evidently, for those clusters the “noncrystalline” geometries were calculated by the extended Thomas-Fermi method of Sec. II, in order to be consistent with the rest of the data displayed in Fig. 8; we stress, however, that the energy of those clusters was obtained after a Kohn-Sham calculation on top of the fixed geometries. The magic number nature of these clusters, originating from their closed electronic shells, is clearly appreciated, for instance, for $N = 20, 58, 92, 138,$ and 232 , which are local minima of the energy versus size function for the disordered clusters. The minima are not evident for the other magic numbers due to the absence of calculations for neighbor sizes.

Overall, we have to conclude that in the size range studied in this paper ($N \leq 340$): (a) the disordered (or noncrystalline) clusters are more stable than the (distorted) crystalline ones. There are certainly cases when the crystalline clusters are very competitive; see, for instance, the competition between crystalline and noncrystalline clusters in the region $N = 130$ – 140 . But even in those extreme cases we only observe competition, but never dominance of crystalline clusters. (b) As a con-

sequence the magic clusters of electronic origin, stabilized by the closing of electronic shells, are more stable than crystalline clusters with closed atomic shells. (c) The competition between crystalline clusters and shell-closing electronic clusters increases with the number of atoms and eventually the crystalline clusters will become more stable,¹⁶ but the crossover appears to occur at a critical size larger than the size predicted by Maiti and Falicov.¹³ In fact, by performing calculations up to $N = 340$ we have not yet found the crossover. Our result is consistent with the experiments of Martin *et al.*¹⁶ for sodium; these authors have observed evidence of crystalline clusters only beyond $N \simeq 1500$.

IV. CONCLUSIONS

Using the density-functional formalism and the SAPS model we have studied the relative stabilities of (a) perfect crystalline sodium clusters with closed atomic shells and optimized lattice constant; (b) distorted-crystalline clusters obtained by a steepest-descent relaxation of the perfect ones; (c) noncrystalline clusters obtained by a full steepest-descent minimization of the total energy starting from random atomic arrangements. The size range studied includes clusters up to $N = 340$. Small distortions from the perfect crystalline structure help to stabilize the cluster and these distorted-crystalline structures compete sometimes with the disordered structures although the disordered clusters are overall the most stable ones. In particular, noncrystalline clusters with closed electronic shells (the well-known electronic magic numbers), are the most stable between all the clusters studied in this paper. From the known relation between thermodynamic stability and abundance in a cluster beam we conclude that the crossover between electronic magic numbers and atomic magic numbers will only be observed for clusters larger than those studied in this paper. Our conclusion is consistent with the experiments of Martin and co-workers,¹⁶ who found evidence for crystalline clusters only for $N \geq 1500$.

ACKNOWLEDGMENTS

This work has been supported by DGICYT (Grant No. PB89-0352-C02-01). M.D.G. acknowledges the Ministerio de Educación y Ciencia of Spain and the Consejo Nacional de Investigaciones Científicas y Técnicas (CONICET) – República Argentina for partial support.

¹W.A. de Heer, W.D. Knight, M.Y. Chou, and M.L. Cohen, in *Solid State Physics*, edited by H. Ehrenreich, F. Seitz, and D. Turnbull (Academic, New York, 1987), Vol. 40, p. 93.

²W. Ekardt, *Phys. Rev. B* **29**, 1558 (1984).

³M.P. Iñiguez, J.A. Alonso, and L.C. Balbás, *Solid State Commun.* **57**, 85 (1986).

⁴M.Y. Chou and M.L. Cohen, *Phys. Lett.* **113A**, 420 (1986).

⁵M.P. Iñiguez, J.A. Alonso, M.A. Aller, and L.C. Balbás, *Phys. Rev. B* **34**, 2152 (1986).

⁶W. Ekardt, *Phys. Rev. B* **37**, 9993 (1988).

⁷S. Bjørnholm, J. Borggreen, O. Echt, K. Hansen, J. Pedersen, and H.D. Rasmussen, *Z. Phys. D* **19**, 47 (1991).

⁸T. Lange, H. Göhlich, T. Bergmann, and T.P. Martin, *Z. Phys. D* **19**, 113 (1991).

⁹M. Brack, O. Genzken, and K. Hansen, *Z. Phys. D* **21**, 65

- (1991).
- ¹⁰H. Nishioka, K. Hansen, and B. Mottelson, *Phys. Rev. B* **42**, 9377 (1990).
- ¹¹K. Clemenger, *Phys. Rev. B* **44**, 12991 (1991).
- ¹²O. Genzken and M. Brack, *Phys. Rev. Lett.* **67**, 3286 (1991).
- ¹³A. Maiti and L.M. Falicov, *Phys. Rev. A* **44**, 4442 (1991).
- ¹⁴J. Pedersen, S. Bjørnholm, J. Borggreen, K. Hansen, T.P. Martin, and H.D. Rasmussen, *Nature* **353**, 733 (1991).
- ¹⁵T.P. Martin, S. Bjørnholm, J. Borggreen, C. Bréchnignac, Ph. Cahuzac, K. Hansen, and J. Pedersen, *Chem. Phys. Lett.* **186**, 53 (1991).
- ¹⁶T.P. Martin, T. Bergmann, H. Göhlich, and T. Lange, *Z. Phys. D* **19**, 25 (1991).
- ¹⁷M.P. Iñiguez, J.M. López, J.A. Alonso, and J.M. Soler, *Z. Phys. D* **11**, 163 (1989).
- ¹⁸M.J. López, M.P. Iñiguez, and J.A. Alonso, *Phys. Rev. B* **41**, 5636 (1990).
- ¹⁹A. Mañanes, M.P. Iñiguez, M.J. López, and J.A. Alonso, *Phys. Rev. B* **42**, 5000 (1990).
- ²⁰M.J. López, M.P. Iñiguez, and J.A. Alonso, *Z. Phys. D* **19**, 141 (1991).
- ²¹R.G. Parr and W. Yang, *Density Functional Theory of Atoms and Molecules* (Oxford University Press, New York, 1989).
- ²²G. Borstel, U. Lammers, A. Mañanes, and J.A. Alonso, in *Nuclear Physics Concepts in Atomic Cluster Physics*, edited by R. Schmidt, H.O. Lutz, and R. Dreizler, *Lecture Notes in Physics* (Springer, Berlin, 1992), p. 327.
- ²³M.D. Glossman, M.P. Iñiguez, and J.A. Alonso, *Z. Phys. D* **22**, 541 (1992).
- ²⁴U. Lammers, G. Borstel, A. Mañanes, and J.A. Alonso, *Z. Phys. D* **17**, 203 (1990).
- ²⁵A. Mañanes, J.A. Alonso, U. Lammers, and G. Borstel, *Phys. Rev. B* **44**, 7273 (1991).
- ²⁶J. Mansikka-aho, M. Manninen, and E. Hammarén, *Z. Phys. D* **21**, 271 (1991).
- ²⁷W. Kohn and L.J. Sham, *Phys. Rev.* **140**, A1133 (1965).
- ²⁸C.F. Weizsäcker, *Z. Phys.* **96**, 431 (1935).
- ²⁹A. Rubio, L.C. Balbás, and J.A. Alonso, *Physica B* **167**, 19 (1990).
- ³⁰P.A.M. Dirac, *Proc. Cambridge Philos. Soc.* **26**, 376 (1930).
- ³¹E.P. Wigner, *Phys. Rev.* **46**, 1002 (1934); *Trans. Faraday Soc.* **34**, 678 (1938).
- ³²N.W. Ashcroft, *Phys. Lett.* **23**, 48 (1966).
- ³³C. Kittel, *Introduction to Solid State Physics* (Wiley, New York, 1971).
- ³⁴A.L. Mackay, *Acta Crystallogr.* **15**, 916 (1962).
- ³⁵M.R. Hoare and P. Pal, *Adv. Phys.* **20**, 61 (1971).
- ³⁶C. Baladrón, M.P. Iñiguez, and J.A. Alonso, *Solid State Commun.* **50**, 549 (1984).